Supplemental Material

Exchange bias and enhanced magnetoelectric effect in $FeNiMo_3O_8$

Junkai Yang,[1,2] Ying Meng,[1,2] Xiangfei Li,[1,2] Luyao Wang,[1,2] Haoyu Zhuang,[1,2] Jie Zhang,[1,2] Xi Shen,[1,†] Youwen Long,[1,2] and Richeng Yu[1,2,3,‡]

[1]*Beijing National Laboratory for Condensed Matter Physics, Institute of Physics, Chinese Academy of Sciences, Beijing 100190, P. R. China*

[2]*School of Physical Sciences, University of Chinese Academy of Sciences, Beijing 100049, P. R. China*

[3]*Songshan Lake Materials Laboratory, Dongguan, Guangdong 523808, P. R. China*

[†]Contact author: xshen@iphy.ac.cn

[‡]Contact author: rcyu@iphy.ac.cn

TABLE S1. Doping ratios in different regions of sample.

	1	2	3	4	5	Average
Fe	47.2%	47.6%	48.0%	47.6%	48.8%	47.8%
Ni	52.8%	52.4%	52.0%	52.4%	51.2%	52.2%

During elemental quantitative analysis, the K_α line detected under 15 kV was adopted.

FIG. S1. Structural characterizations of $FeNiMo_3O_8$, with SAED pattern observed along the [100] zone axis.

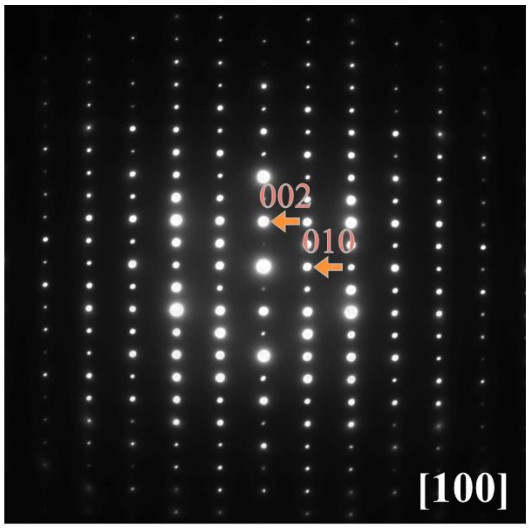

TABLE S2. Data collection and structure refinement of FNMO

Crystal data		Data collection	
Formula	$(Fe_{0.49}Ni_{0.51})_2Mo_3O_8$	Temperature	273(2) K
Space group	*P*6$_3$*mc* (No. 186)	Wavelength	0.71073 Å
a, b	5.7706(3) Å	μ	12.023 mm^{-1}
c	9.9159(5) Å	F(000)	485
α, β	90°		$-7 \leq h \leq 7$
γ	120°	Index ranges	$-7 \leq k \leq 7$
Volume	285.96(3) $Å^3$		$-13 \leq l \leq 13$
ρ_{calc}	6.114 g/cm^3	Reflection collected	3790
R_1	1.41%	Independent reflection	316
wR_2	3.36%	Parameters	34
S	1.099	Largest diff. peak and hole	0.46/−0.54 $eÅ^{-3}$

Structural information was obtained from the refinement by the SHELXL program.

TABLE S3. Positions of atoms in FNMO, determined from SCXRD.

Atom	*x*	*y*	*z*	Occupancy	U (Å$^2 \times 10^3$)
Ni(1)	1/3	2/3	0.63063(14)	0.987	5.9(3)
Fe(2)	2/3	1/3	0.56870(18)	0.970	6.9(5)
Ni(2)	2/3	1/3	0.56869(18)	0.030	6.9(5)
Mo	0.14617(4)	0.29233(9)	0.36838(6)	0.988	4.09(19)
O(1)	0.4866(5)	0.5134(5)	0.4849(5)	1	6.4(9)
O(2)	0	0	0.5096(7)	1	8.4(14)
O(3)	1/3	2/3	0.2656(8)	1	5.1(15)
O(4)	0.3362(9)	0.1681(4)	0.2524(7)	1	6.8(11)

SCXRD refinement on FNMO. A total of 3790 Bragg peaks are collected and refined with a space group $P6_3mc$. The refinement residuals $R_1 = 1.41\%$, $wR_2 = 3.36\%$, and $S = 1.099$.

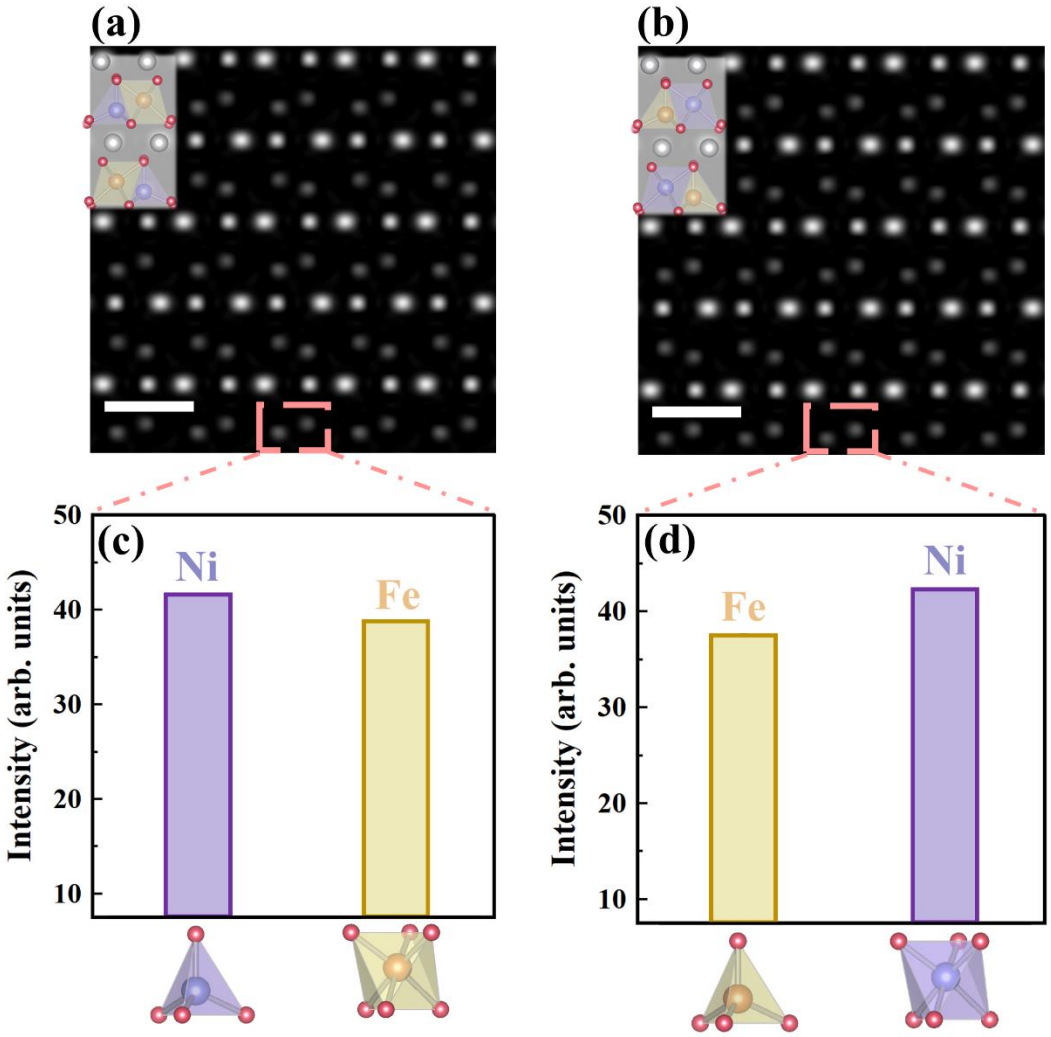

FIG. S2. HAADF simulation images for two structural models. ((a), (b)) HAADF simulation images for two different occupancy structural models, with corresponding structural models overlaid in the upper left corner, where yellow and purple spheres represent Fe and Ni atoms, respectively. Simulation parameters refer to those under actual experimental conditions: sample thickness 30 nm, defocus 10 nm, acceleration voltage 300 kV, convergence semi-angle of 24 mrad, and collection angle of 54−220 mrad. The scale bar in the image is 0.5 nm. (c) and (d) Intensity distributions within the dashed boxes in panels (a) and (b), respectively with corresponding elements marked below the signal peaks.

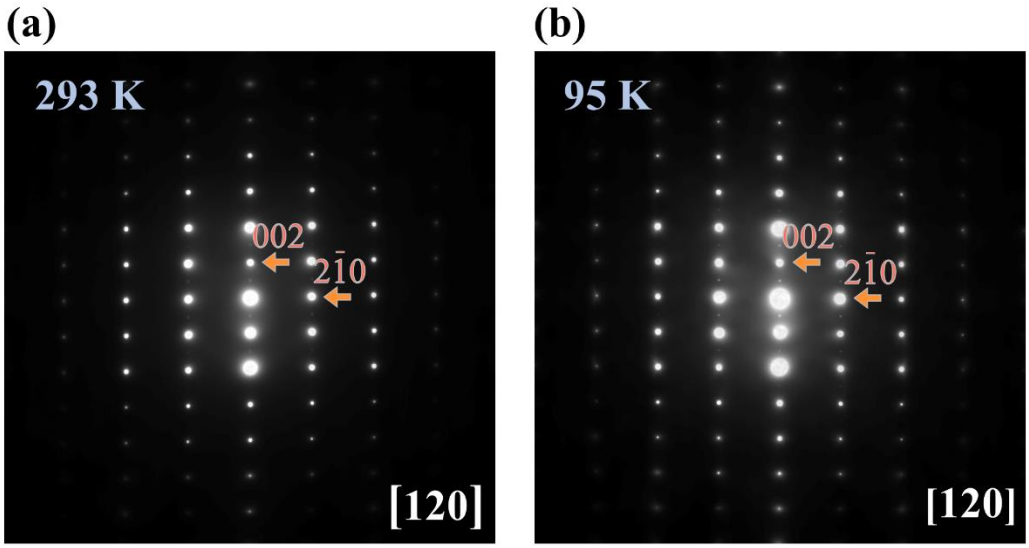

FIG. S3. SAED patterns of FNMO along the [120] direction taken at (a) 293 K and (b) 95 K, respectively, with indexed information of diffraction spots marked in the figures.

TABLE S4. Variation of lattice constants with temperature.

T (K)	a (Å)	c (Å)	c / a	V (Å^3)
293	5.75	9.92	1.73	284
95	5.88	10.11	1.72	303

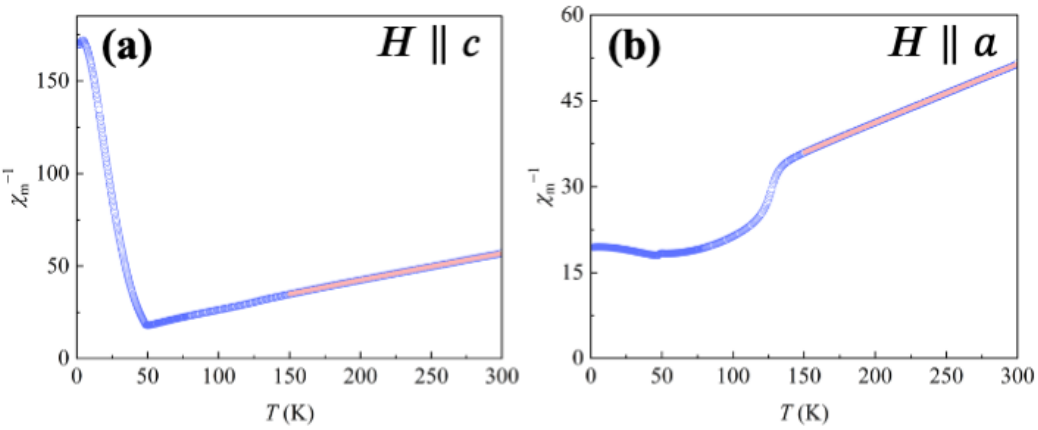

FIG. S4. (a) and (b) show the Curie–Weiss fitting results along the *c*-axis and *a*-axis, respectively. The blue dots represent the original measured data, while the pink lines indicate the high-temperature fitting results.

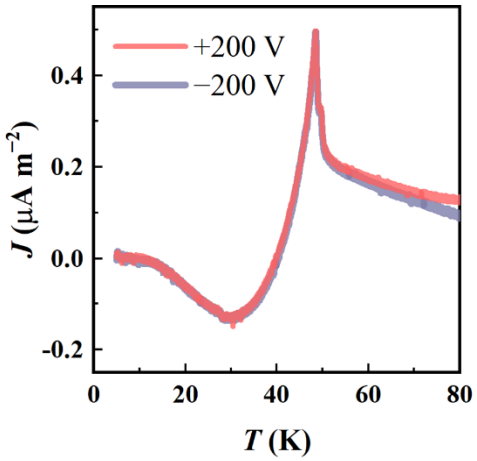

FIG. S5. Pyroelectricity of FNMO. Prior to the measurement, a pre-polarization electric field is applied to the sample in the cooling process (200−5 K).

TABLE S5. Calculation of ligand field stabilization energy.

	$\mathrm{LFSE_O}$	$\mathrm{LFSE_T}$	$\mathrm{LFSE_O} - \mathrm{LFSE_T}$
$\mathrm{Fe^{2+}}(d^6)$	$-\frac{2}{5}\Delta_\mathrm{O}$	$-\frac{3}{5}\Delta_\mathrm{T}$	$-\frac{6}{45}\Delta_\mathrm{O}$
$\mathrm{Ni^{2+}}(d^8)$	$-\frac{6}{5}\Delta_\mathrm{O}$	$-\frac{4}{5}\Delta_\mathrm{T}$	$-\frac{38}{45}\Delta_\mathrm{O}$

When the same ligands are employed, $\Delta_\mathrm{T} \approx \frac{4}{9}\Delta_\mathrm{O}$. This ratio is inferred from the angular overlap approach.

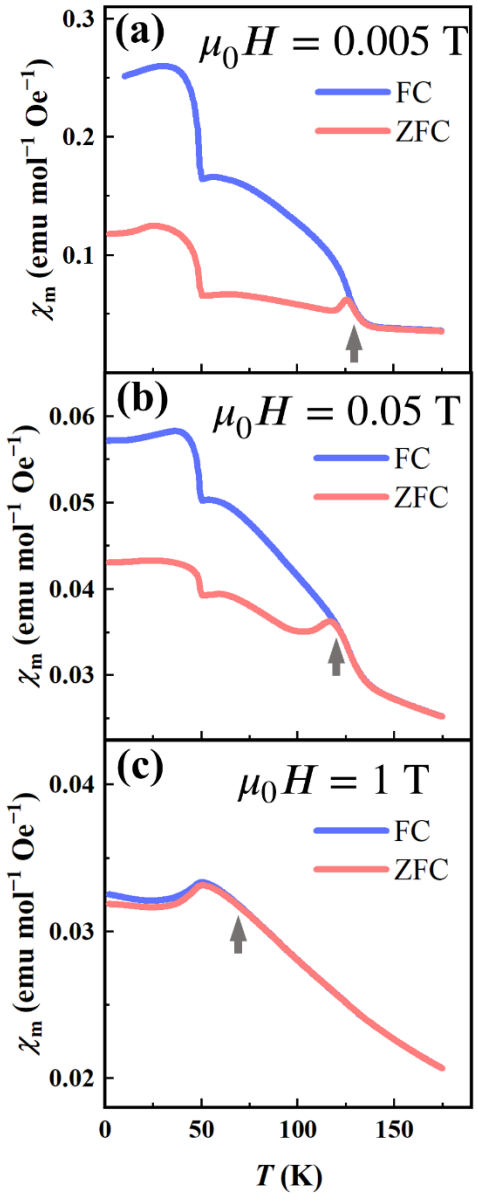

FIG. S6. Variations of DC susceptibility with temperature, measured under (a) 0.005 T, (b) 0.05 T, and (c) 1 T, respectively, with arrows marked the temperature where the FC and ZFC curves bifurcate.